

# Langevin Simulation of Scalar Fields: Additive and Multiplicative Noises and Lattice Renormalization

N. C. Cassol-Seewald,<sup>1,\*</sup> R. L. S. Farias,<sup>2,†</sup> E. S. Fraga,<sup>3,‡</sup> G. Krein,<sup>1,§</sup> and Rudnei O. Ramos<sup>2,¶</sup>

<sup>1</sup>*Instituto de Física Teórica, Universidade Estadual Paulista, 01405-900 São Paulo, SP, Brazil*

<sup>2</sup>*Departamento de Física Teórica, Universidade do Estado do Rio de Janeiro, 20550-013 Rio de Janeiro, RJ, Brazil*

<sup>3</sup>*Instituto de Física, Universidade Federal do Rio de Janeiro, 21941-972 Rio de Janeiro, RJ, Brazil*

We consider the nonequilibrium dynamics of the formation of a condensate in a spontaneously broken  $\lambda\phi^4$  scalar field theory, incorporating additive and multiplicative noise terms to study the role of fluctuation and dissipation. The corresponding stochastic Ginzburg-Landau-Langevin (GLL) equation is derived from the effective action, and solved on a  $(3+1)$ -dimensional lattice. Particular attention is devoted to the renormalization of the stochastic GLL equation in order to obtain lattice-independent equilibrium results.

PACS numbers: 11.10.Wx, 98.80.Cq, 05.70.Ln

## I. INTRODUCTION

The importance of the investigation of phase transitions under extreme conditions was recognized long ago [1], and efforts were devoted to develop a description within relativistic quantum field theory at finite temperature [2, 3, 4]. Among the variety of phenomena associated with the dynamics of phase transitions, phase ordering seems to be of particular importance for the understanding of the time scales governing the equilibration of systems driven out of equilibrium. The influence of the presence of a hot and dense medium on the dynamics of particles and fields is encoded “macroscopically” in attributes that enter stochastic evolution equations, usually in the form of dissipation and noise terms. Relevant time scales for different stages of phase conversion can depend dramatically on the details of these attributes. In particular, in high-energy heavy ion collisions, where one presumably forms a hot, dense, strongly interacting quark-gluon plasma [5], chiral fields evolve under extreme conditions of temperature and energy density during the QCD phase transition. To have a clear understanding of data coming from BNL-RHIC, and especially of data that will be produced at CERN-LHC, one needs a realistic description of the hierarchy of scales associated with dissipation, noise and radiation, and also with the expansion and finite size of the system.

Some of us have considered the effects of dissipation in the scenario of explosive spinodal decomposition (i.e., the rapid growth of unstable modes following a quench into the two-phase region of the phase diagram) for hadron production [6, 7, 8, 9] during the QCD chiral transition after a high-energy heavy ion collision in the simplest fashion [10]. Using a phenomenological Langevin description inspired by microscopic nonequilibrium field theory results [11, 12, 13], the time evolution of the order parameter in a chiral effective model [14] was investigated. Real-time  $(3+1)$ -dimensional lattice simulations for the behavior of the inhomogeneous chiral fields were performed, and it was shown that the effects of dissipation could be dramatic in spite of the very conservative assumptions that were made. In fact, even if the system quickly reaches the unstable region there is still no guarantee that the unstable modes will grow fast enough. In particular, in the case of hadronization at RHIC time scales, the explosive scenario becomes rather constrained. More recently, analogous but even stronger effects were obtained in the case of the deconfining transition of  $SU(2)$  pure gauge theories using the same approach [15, 16].

The framework for the dynamics was assumed to be given by the following standard GLL equation

$$\square\phi + \eta\dot{\phi} + \mathcal{V}'_{eff}(\phi) = \xi(\mathbf{x}, t), \quad (1.1)$$

where  $\phi$  is a real scalar field (the condensate  $\langle\phi\rangle$  plays the role of the order parameter),  $\mathcal{V}'_{eff}(\phi)$  is the field derivative of a Ginzburg-Landau effective potential and  $\eta$ , which can be seen as a response coefficient that defines time scales for the system and encodes the intensity of dissipation, is usually taken to be a function of temperature only,  $\eta = \eta(T)$ .

---

\*Electronic address: nadiane@ift.unesp.br

†Electronic address: ricardosonegofarias@gmail.com

‡Electronic address: fraga@if.ufrj.br

§Electronic address: gkrein@ift.unesp.br

¶Electronic address: rudnei@uerj.br

The function  $\xi(\mathbf{x}, t)$  represents a stochastic (noise) force, assumed Gaussian and white, so that  $\langle \xi(\mathbf{x}, t) \rangle = 0$  and  $\langle \xi(\mathbf{x}, t) \xi(\mathbf{x}', t') \rangle = 2\eta T \delta(\mathbf{x} - \mathbf{x}') \delta(t - t')$ , in conformity with the fluctuation-dissipation theorem.

However, a more complete field-theory description of nonequilibrium dissipative dynamics [11] shows that the complete form for the effective GLL equation of motion can lead to much more complicated scenarios than the one described by Eq. (1.1), depending on the allowed interaction terms involving  $\phi$ . In general, there will be nonlocal (non-Markovian) dissipation and colored noise, as well as the possibility of field-dependent (multiplicative) noise terms  $\sim \phi \xi$  accompanied by density-dependent dissipation terms. In fact, on very general physical grounds, one expects that dissipation effects should depend on the local density  $\sim \phi^2 \dot{\phi}$  and, accordingly, the noise term should contain a multiplicative piece  $\sim \phi$ . The typical term coming from fluctuations in the equation of motion for  $\phi$  will be a functional of the form

$$\mathcal{F}[\phi(x)] = \phi(x) \int d^4x' \phi^2(x') K_1(x, x') + \int d^4x' \phi(x') K_2(x, x'), \quad (1.2)$$

where  $K_1(x, x')$  and  $K_2(x, x')$  are nonlocal kernels expressed in terms of retarded Green's functions and whose explicit form depends on the detailed nature of the interactions involving  $\phi$ . Explicit treatments for these nonlocal kernels show that under appropriate conditions one is justified to express the effective equation of motion for  $\phi$  in a local form [17, 18, 19, 20, 21]. The existence of these additional terms in the GLL equation will, of course, play an important role in the dynamics of the formation of condensates. For instance, it was recently shown that the effects of multiplicative noise are rather significant in the Kibble-Zurek scenario of defect formation in one spatial dimension [22].

In this paper we consider the nonequilibrium dynamics of the formation of a condensate in a spontaneously broken  $\lambda\phi^4$  scalar field theory within an improved Langevin framework which includes the effects of multiplicative noise and density-dependent dissipation terms. The corresponding stochastic GLL equation is derived in detail from the effective action, generalizing the results of Ref. [11] to the case of broken symmetry. The time evolution for the formation of the condensate, under the influence of additive and multiplicative noise terms, is solved numerically on a  $(3+1)$ -dimensional lattice. Particular attention is devoted to the renormalization of the stochastic GLL equation in order to obtain lattice-independent equilibrium results.

The paper is organized as follows. In Section II we review the perturbative approach of Ref. [11], describe the effective theory that we consider, and present the computation of the effective action up to two loops in the Schwinger-Keldysh closed-time-path formalism, appropriate for a nonequilibrium situation. All results are extended to the case of spontaneously broken symmetry. In Sec. III we discuss the derivation of stochastic GLL equations with additive and multiplicative noises yielded by quantum corrections for a scalar  $\lambda\phi^4$  theory in the symmetric and broken symmetry phases. In Section IV the important issue regarding the proper lattice renormalization of the effective potential in order to achieve equilibrium solutions that are independent of lattice spacing is addressed. In Sec. V we show the results of our lattice simulations to study the behavior of the condensate. Section VI contains our conclusions and perspectives. One appendix is included in order to provide some technical details used in the paper.

## II. EFFECTIVE ACTION UP TO TWO LOOPS

Here we compute the effective equation of motion obtained in Ref. [11] for the symmetric phase, but instead of repeating the derivation in this reference, we make use of a more general method [23, 24] that is valid for both symmetric and broken phases of the theory. The derivation can be easily extended to other field theoretic models.

Let  $S[\phi]$  be the classical action of a real scalar field  $\phi$ ,

$$S[\phi] = \int d^4x \mathcal{L}(\phi), \quad (2.1)$$

with a Lagrangian density  $\mathcal{L}(\phi)$  given by

$$\mathcal{L}(\phi) = \frac{1}{2} (\partial_\mu \phi)^2 - \frac{m_0^2}{2} \phi^2 - \frac{\lambda}{4!} \phi^4, \quad (2.2)$$

where  $m_0^2 = m^2 > 0$  in the symmetric phase and  $m_0^2 = -m^2 < 0$  in the broken phase. In the presence of an external source  $J(x)$  that couples linearly to the field  $\phi$ , the classical action of the theory becomes

$$S[\phi, J] = S[\phi] + \int d^4x J(x) \phi(x). \quad (2.3)$$

The corresponding generating functional  $Z[J]$  is given by

$$Z[J] = \exp \frac{i}{\hbar} W[J] = \int_c \mathcal{D}\phi \exp \frac{i}{\hbar} S_c[\phi, J], \quad (2.4)$$

where the index  $c$  means that we perform our derivation in the context of the real-time Schwinger-Keldysh closed-time path formalism. In this formalism, the time integration is performed along a contour  $C$  with a branch  $C_+$  that goes from  $-\infty$  to  $+\infty$ , and another branch,  $C_-$ , that goes back to  $-\infty$  [26, 27]. The fields and sources on the branch  $C_+$  are denoted  $\phi_+$  and  $J_+$ , and those on the branch  $C_-$  are denoted  $\phi_-$  and  $J_-$ . Therefore,  $S_c[\phi, J]$  in Eq. (2.4) means

$$S_c[\phi, J] = S[\phi_+, J_+] - S[\phi_-, J_-]. \quad (2.5)$$

Our interest is the nonequilibrium effective action  $\Gamma[\varphi]$ , which is a functional of a  $c$ -number field  $\varphi(x)$  containing all quantum effects. It is defined through the Legendre transformation

$$\Gamma[\varphi] = W[J] - (J\varphi)_c, \quad (2.6)$$

where  $\varphi(x)$  is given by

$$\varphi(x) = \frac{\delta W[J(x)]}{\delta J(x)}. \quad (2.7)$$

For convenience we have introduced the notation

$$(J\phi)_c = \int_c d^4x J(x) \phi(x). \quad (2.8)$$

The external source can now be eliminated in favor of  $\varphi$  through

$$J(x) = -\frac{\delta \Gamma[\varphi]}{\delta \varphi(x)} \equiv -\Gamma_1[\varphi]. \quad (2.9)$$

The quantum effects encoded in  $\varphi$  can be made explicit by an expansion in powers of  $\hbar$ , the loop expansion, which can be implemented in the following way [28]. One starts by making the shift in the field variable  $\phi$

$$\phi(x) \rightarrow \phi(x) + \varphi(x) \quad (2.10)$$

in the functional integral of Eq. (2.4), so that

$$\exp \frac{i}{\hbar} \Gamma[\varphi] = \int_c \mathcal{D}\phi \exp \frac{i}{\hbar} [S_c[\phi + \varphi] - (\Gamma_1[\varphi]\phi)_c], \quad (2.11)$$

where we have used Eq. (2.9) to eliminate  $J$ . Next, one expands  $S[\phi + \varphi]$  around  $\phi = 0$  obtaining

$$S_c[\phi + \varphi] = S[\varphi] + \sum_{n=1}^{\infty} \frac{1}{n!} (S_n[\varphi]\phi^n)_c, \quad (2.12)$$

where  $S[\varphi]$  is the classical action and

$$(S_n[\varphi]\phi^n)_c = \int_c d^4x_1 \cdots d^4x_n S_n[\varphi] \phi(x_1) \cdots \phi(x_n), \quad (2.13)$$

with

$$S_n[\varphi] = \left[ \frac{\delta^n S[\phi + \varphi]}{\delta \phi(x_1) \cdots \delta \phi(x_n)} \right]_{\phi=0}. \quad (2.14)$$

Then we substitute this into Eq. (2.11):

$$\begin{aligned} \exp \frac{i}{\hbar} \bar{\Gamma}[\varphi] &= \int_c \mathcal{D}\phi \exp \frac{i}{\hbar} \left[ \frac{1}{2} (S_2[\varphi]\phi^2)_c \right. \\ &\quad \left. + \sum_{n=3}^{+\infty} \frac{1}{n!} (S_n[\varphi]\phi^n)_c - (\bar{\Gamma}_1[\varphi]\phi)_c \right], \end{aligned} \quad (2.15)$$

where we have made explicit the term quadratic (in  $\phi$ ) in the exponent of the functional integral, and have defined

$$\bar{\Gamma}[\varphi] = \Gamma[\varphi] - S[\varphi], \quad (2.16)$$

and equivalently for the combination  $\Gamma_1[\varphi] - S_1[\varphi]$ .

Now, to make explicit the  $\hbar$  dependence of the different terms in the expansion in Eq. (2.15) we rescale  $\phi$  as  $\phi \rightarrow \hbar^{1/2}\phi$  and expand  $\bar{\Gamma}[\varphi]$  and  $\bar{\Gamma}_1[\varphi]$  in powers of  $\hbar$ ,

$$\bar{\Gamma}[\varphi] = \sum_{n=1}^{\infty} \hbar^n \bar{\Gamma}^{(n)}[\varphi], \quad \bar{\Gamma}_1[\varphi] = \sum_{n=1}^{\infty} \hbar^n \bar{\Gamma}_1^{(n)}[\varphi], \quad (2.17)$$

to obtain the final result:

$$\exp i \sum_{n=1}^{\infty} \hbar^{n-1} \bar{\Gamma}^{(n)}[\varphi] = \int_c \mathcal{D}\phi \exp i \left[ \frac{1}{2} (S_2[\varphi]\phi^2)_c + \sum_{n=3}^{\infty} \frac{\hbar^{n/2-1}}{n!} (S_n[\varphi]\phi^n)_c - \sum_{n=1}^{\infty} \hbar^{n-1/2} (\bar{\Gamma}_1^{(n)}[\varphi]\phi)_c \right]. \quad (2.18)$$

The functional  $\bar{\Gamma}[\varphi]$  carries all the quantum corrections to the classical action  $S[\varphi]$ , without any approximation. In the following we consider the one- and two-loop contributions to the effective action. These are obtained by expanding both sides of Eq. (2.18) in powers of  $\hbar$  and equating terms of the same order. Specifically, the one-loop contribution is given by

$$\bar{\Gamma}^{(1)}[\varphi] = -i \ln \int_c \mathcal{D}\phi \exp \frac{i}{2} (S_2\phi^2)_c. \quad (2.19)$$

Since the exponential is quadratic in  $\phi$ , the functional integral in principle can be calculated exactly. However, in order to obtain an useful expression for deriving an effective GLL equation, we perform a perturbative calculation. This will be done in the next subsection.

The two-loop contribution to the effective action is obtained keeping terms up to first order in  $\hbar$  in the expansion of both sides of Eq. (2.18). The contributing terms are given by

$$\exp i \left( \bar{\Gamma}^{(1)}[\varphi] + \hbar \bar{\Gamma}^{(2)}[\varphi] \right) = \int_c \mathcal{D}\phi \exp i \left[ \frac{1}{2} (S_2[\varphi]\phi^2)_c + \frac{\hbar^{1/2}}{3!} (S_3[\varphi]\phi^3)_c + \frac{\hbar}{4!} (S_4[\varphi]\phi^4)_c - \hbar^{1/2} (\bar{\Gamma}_1^{(1)}[\varphi]\phi)_c \right]. \quad (2.20)$$

Expanding the  $\hbar$ -dependent exponentials on both sides of this equation, keeping  $\mathcal{O}(\hbar)$  terms, and using Eq. (2.19) for  $\bar{\Gamma}^{(1)}[\varphi]$  into this last equation, one obtains for  $\bar{\Gamma}^{(2)}[\varphi]$  the following expression:

$$\bar{\Gamma}^{(2)}[\varphi] = \frac{i}{2(3!)^2} \langle (S_3[\varphi]\phi^3)_c (S_3[\varphi]\phi^3)_c \rangle_c + \frac{1}{4!} \langle (S_4[\varphi]\phi^4)_c \rangle_c + \frac{i}{2} \langle (\Gamma_1^{(1)}[\varphi]\phi)_c (\Gamma_1^{(1)}[\varphi]\phi)_c \rangle_c - \frac{i}{3!} \langle (S_3[\varphi]\phi^3)_c (\bar{\Gamma}_1^{(1)}[\varphi]\phi)_c \rangle_c, \quad (2.21)$$

where the angular brackets  $\langle F(\phi) \rangle_c$  mean

$$\langle F(\phi) \rangle_c = \frac{\int_c \mathcal{D}\phi F(\phi) \exp \left( \frac{i}{2} S_2[\varphi]\phi^2 \right)_c}{\int_c \mathcal{D}\phi \exp \left( \frac{i}{2} S_2[\varphi]\phi^2 \right)_c}. \quad (2.22)$$

### A. Perturbative expansion of $\bar{\Gamma}^{(1)}[\varphi]$

So far, our treatment has been completely general in the sense that no differentiation between symmetric and broken phases has been done. However, for the implementation of a perturbative expansion it is necessary to make sure that the perturbation is performed around a stable field configuration. In order to ensure this situation and still keep treating both phases on the same footing we consider  $\varphi(x)$  as

$$\varphi(x) \rightarrow \nu + \varphi(x) \quad (2.23)$$

where  $\nu$  is a  $x$ -independent field configuration. At tree level, in the broken phase where  $m_0^2 = -m^2 < 0$  in Eq. (2.2), one has  $\nu = \nu_0$  with  $\nu_0^2 = 6m^2/\lambda$ , whereas  $\nu = 0$  in the symmetric phase. In the following, though, we will not use the tree value of  $\nu$ . Instead, we determine it through the long-time behavior of the solution of the corresponding effective GLL equation. As we will show later, in the the symmetric phase  $\nu = 0$ , and in the broken phase  $\nu \simeq \nu_0$  for couplings not very large – which should be the case for the validity of the perturbative expansion.

For the evaluation of the one-loop expression for the effective action, Eq. (2.19), one needs the quadratic action ( $S_2[\varphi]\phi^2$ ), where  $S_2[\varphi]$  is defined in Eq. (2.14). We organize the perturbative expansion in a way that

$$S_2[\varphi] = iS^0(x_1 - x_2) - \lambda V''(\varphi(x_1)) \delta^{(4)}(x_1 - x_2), \quad (2.24)$$

where

$$S^0(x_1 - x_2) = -i(-\square_{x_1} - \mu^2) \delta^{(4)}(x_1 - x_2), \quad (2.25)$$

and

$$V''(\varphi) = \frac{1}{2} \varphi^2 + \nu \varphi, \quad (2.26)$$

with

$$\mu^2 = -m^2 + \frac{1}{2} \lambda \nu^2. \quad (2.27)$$

Therefore, one can write for  $\Gamma^{(1)}[\varphi]$  the expression

$$\begin{aligned} \Gamma^{(1)}[\varphi] &= S[\varphi] - i \ln \int_c \mathcal{D}\phi \exp \frac{1}{2} (S^0 \phi^2)_c \\ &\times \exp \left[ -i \frac{1}{2} \lambda \int_c d^4 x V''(\varphi(x)) \phi^2(x) \right], \end{aligned} \quad (2.28)$$

and the perturbative series is obtained from the expansion of the second exponential in powers of  $\lambda$ . Specifically, defining

$$Z = \int_c \mathcal{D}\phi \exp \frac{1}{2} (S^0 \phi^2)_c, \quad (2.29)$$

and

$$\langle F(\phi) \rangle_c^0 = \frac{1}{Z} \int_c \mathcal{D}\phi F(\phi) \exp \frac{1}{2} (S^0 \phi^2)_c, \quad (2.30)$$

one obtains up to  $\mathcal{O}(\lambda^2)$

$$\Gamma^{(1)}[\varphi] = S[\varphi] - i \ln Z - \frac{\lambda}{2} \int_c d^4 x V''(\varphi(x)) \langle \phi^2(x) \rangle_c^0 + i \frac{\lambda^2}{4} \int_c d^4 x V''(\varphi(x)) \int_c d^4 y V''(\varphi(y)) [\langle \phi(x) \phi(y) \rangle_c^0]^2. \quad (2.31)$$

To proceed one needs to make explicit the correlation functions  $\langle \phi(x) \phi(y) \rangle_c^0$  on  $C_+$  and  $C_-$ . There are four of such correlation functions,  $G_0^{\alpha\beta}(x - x')$  with  $\alpha, \beta = \pm$ .  $G_0^{++}$  is the correlation function of  $\phi(x)$  and  $\phi(y)$  when both fields are on the branch  $C_+$  of the Schwinger-Keldysh contour, and therefore is the usual time-ordered propagator.  $G_0^{--}$  is for both fields on  $C_-$ , and gives rise to an anti-time-ordered correlation function. The  $G_0^{+-}$  and  $G_0^{-+}$  refer to correlations of one field on one branch and one on the other branch.  $G_0^{++}$  is the usual physical (causal) propagator; the other three come as a consequence of the time contour, and are auxiliary quantities [29]. In the above, the subindex 0 means that these correlation functions are calculated with the action  $S^0$ , defined in Eq. (2.25). All four  $G_0^{\alpha\beta}$  can be expressed in terms of the usual advanced  $G_0^>(\mathbf{x}, t)$  and retarded  $G_0^<(\mathbf{x}, t)$  correlation functions as

$$\begin{aligned} G_0^{++}(\mathbf{x}, t) &= G_0^>(\mathbf{x}, t) \theta(t) + G_0^<(\mathbf{x}, t) \theta(-t), \\ G_0^{--}(\mathbf{x}, t) &= G_0^>(\mathbf{x}, t) \theta(-t) + G_0^<(\mathbf{x}, t) \theta(t), \\ G_0^{+-}(\mathbf{x}, t) &= G_0^<(\mathbf{x}, t), \\ G_0^{-+}(\mathbf{x}, t) &= G_0^>(\mathbf{x}, t). \end{aligned} \quad (2.32)$$

From now on, it is convenient to consider the spatial Fourier transforms of  $G_0^{\alpha\beta}(\mathbf{x}, t)$ , defined as

$$G_0^{\alpha\beta}(\mathbf{x}, t) = i \int \frac{d^3 k}{(2\pi)^3} e^{i\mathbf{k}\cdot\mathbf{x}} G_0^{\alpha\beta}(\mathbf{k}, t). \quad (2.33)$$

The  $i$  on the r.h.s. of this equation is introduced for convenience, so that  $G_0^{\alpha\beta}(\mathbf{k}, t)$  becomes real. In terms of these Fourier transforms, and making use of Eq. (2.32) to express the  $G_0^>$  in terms of  $G_0^>$  and  $G_0^<$ , the expression for  $\Gamma^{(1)}[\varphi]$  can be written as

$$\begin{aligned}
\Gamma^{(1)}[\varphi] = & S[\varphi] - \frac{\lambda}{2} \int d^4x \int \frac{d^3k}{(2\pi)^3} \left( V''(\varphi_+(x)) - V''(\varphi_-(x)) \right) G_0^{++}(\mathbf{k}, 0) \\
& + i \frac{\lambda^2}{4} \int_{-\infty}^{\infty} d^4x d^4x' \int \frac{d^3q}{(2\pi)^3} \int \frac{d^3k}{(2\pi)^3} e^{i\mathbf{k} \cdot (\mathbf{x} - \mathbf{x}')} \left[ V''(\varphi_+(x)) V''(\varphi_+(x')) G_0^{++}(\mathbf{q}, \Delta t) G_0^{++}(\mathbf{q} - \mathbf{k}, \Delta t) \right. \\
& - V''(\varphi_+(x)) V''(\varphi_-(x')) G_0^{+-}(\mathbf{q}, \Delta t) G_0^{+-}(\mathbf{q} - \mathbf{k}, \Delta t) - V''[\varphi_-(x)] V''[\varphi_+(x')] G_0^{-+}(\mathbf{q}, \Delta t) G_0^{-+}(\mathbf{q} - \mathbf{k}, \Delta t) \\
& \left. + V''[\varphi_-(x)] V''(\varphi_-(x')) G_0^{--}(\mathbf{q}, \Delta t) G_0^{--}(\mathbf{q} - \mathbf{k}, \Delta t) \right], \quad (2.34)
\end{aligned}$$

where  $\Delta t = t - t'$ . To proceed, one needs explicit expressions for  $G^{\alpha\beta}$ . This will be discussed in Section III, after we present the perturbative expansion for  $\bar{\Gamma}^{(2)}[\varphi]$  in the following.

### B. Perturbative expansion of $\bar{\Gamma}^{(2)}[\varphi]$

Since  $(S_2[\varphi]\phi^2)$  in Eq. (2.22) is quadratic, one can apply Wick's theorem and, after straightforward manipulations, one obtains the following terms that contribute to the expansion of  $\bar{\Gamma}^{(2)}[\varphi]$  up to  $\mathcal{O}(\lambda^2)$

$$\bar{\Gamma}^{(2)}[\varphi] = -\frac{\lambda}{8} \int_c d^4x V''''(\varphi) [\langle \phi^2(x) \rangle]^2 + \bar{\Gamma}_{\text{setting-sun}}^{(2)}[\varphi], \quad (2.35)$$

where

$$\begin{aligned}
\bar{\Gamma}_{\text{setting-sun}}^{(2)}[\varphi] = & i \frac{\lambda^2}{12} \int_c d^4x V''''(\varphi(x)) \\
& \times \int_c d^4y V''''(\varphi(y)) [\langle \phi(x)\phi(y) \rangle_0]^3. \quad (2.36)
\end{aligned}$$

and

$$V''''(\varphi) = \varphi + \nu, \quad V''''(\varphi) = 1. \quad (2.37)$$

To complete the  $\mathcal{O}(\lambda^2)$  expansion, one needs  $\langle \phi(x)\phi(y) \rangle$  up to first order in  $\lambda$ . This is given by

$$\langle \phi(x)\phi(y) \rangle = \langle \phi(x)\phi(y) \rangle_0 - i\lambda \int_c d^4z V''(\varphi(z)) \langle \phi(x)\phi(z) \rangle_0 \langle \phi(y)\phi(z) \rangle_0. \quad (2.38)$$

Substituting this into the expression for  $\bar{\Gamma}^{(2)}[\varphi]$  in Eq. (2.36), one obtains

$$\bar{\Gamma}^{(2)}[\varphi] = -\frac{\lambda}{8} \int_c d^4x V''''(\varphi) [\langle \phi^2(x) \rangle_0]^2 + \bar{\Gamma}_{\text{snow-man}}^{(2)}[\varphi] + \bar{\Gamma}_{\text{setting-sun}}^{(2)}[\varphi], \quad (2.39)$$

where

$$\bar{\Gamma}_{\text{snow-man}}^{(2)}[\varphi] = i \frac{\lambda^2}{4} \int_c d^4x V''''(\varphi) [\langle \phi^2(x) \rangle_0] \int_c d^4x' V''(\varphi(x')) [\langle \phi(x)\phi(x') \rangle_0]^2. \quad (2.40)$$

Using now the Fourier transforms of  $G^{\alpha\beta}$ , and following the same procedure as in the previous subsection of regrouping terms after using the expressions in Eq. (2.32), one obtains after a lengthy but straightforward calculation the following expression for  $\bar{\Gamma}_{\text{snow-man}}^{(2)}[\varphi]$ :

$$\begin{aligned}
\bar{\Gamma}_{\text{snow-man}}^{(2)}[\varphi] = & \frac{i\lambda^2}{4} \int d^4x dt' \int \frac{d^3k}{(2\pi)^3} \int \frac{d^3q}{(2\pi)^3} V''''(\varphi) G_0^{++}(\mathbf{k}, 0) \left\{ V''[\varphi_+(x)] [G_0^{++}(\mathbf{q}, \Delta t)]^2 \right. \\
& \left. - V''[\varphi_-(x)] [G_0^{-+}(\mathbf{q}, \Delta t)]^2 - V''[\varphi_+(x)] [G_0^{+-}(\mathbf{q}, \Delta t)]^2 + V''[\varphi_-(x)] [G_0^{--}(\mathbf{q}, \Delta t)]^2 \right\}, \quad (2.41)
\end{aligned}$$

where we used the fact that  $V''''(\varphi_+) = V''''(\varphi_-) = V''''(\varphi)$ , in view of Eq. (2.37). In the same way, one obtains for  $\bar{\Gamma}_{\text{setting-sun}}^{(2)}[\varphi]$ :

$$\begin{aligned} \bar{\Gamma}_{\text{setting-sun}}^{(2)}[\varphi] = & \frac{i\lambda^2}{12} \int d^4x d^4x' \int d^3k e^{i\mathbf{k}\cdot(\mathbf{x}-\mathbf{x}')} \int \frac{d^3q_1}{(2\pi)^3} \int \frac{d^3q_2}{(2\pi)^3} \int \frac{d^3q_3}{(2\pi)^3} \delta^3(\mathbf{k} - \mathbf{q}_1 - \mathbf{q}_2 - \mathbf{q}_3) \\ & \times \left\{ V''''[\varphi_+(x)] V''''[\varphi_+(x')] G_0^{++}(\mathbf{q}_1, \Delta t) G_0^{++}(\mathbf{q}_2, \Delta t) G_0^{++}(\mathbf{q}_3, \Delta t) \right. \\ & - V''''[\varphi_+(x)] V''''[\varphi_-(x')] G_0^{+-}(\mathbf{q}_1, \Delta t) G_0^{+-}(\mathbf{q}_2, \Delta t) G_0^{+-}(\mathbf{q}_3, \Delta t) \\ & - V''''[\varphi_-(x)] V''''[\varphi_+(x')] G_0^{-+}(\mathbf{q}_1, \Delta t) G_0^{-+}(\mathbf{q}_2, \Delta t) G_0^{-+}(\mathbf{q}_3, \Delta t) \\ & \left. + V''''[\varphi_-(x)] V''''[\varphi_-(x')] G_0^{--}(\mathbf{q}_1, \Delta t) G_0^{--}(\mathbf{q}_2, \Delta t) G_0^{--}(\mathbf{q}_3, \Delta t) \right\}. \end{aligned} \quad (2.42)$$



Figure 1: Contributions to the finite-temperature effective action in the symmetric phase up to two loops and  $\mathcal{O}(\lambda^2)$ .

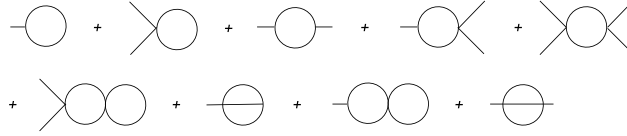


Figure 2: Contributions to the finite-temperature effective action, in the broken phase, up to two loops and  $\mathcal{O}(\lambda^2)$ .

In Figs. 1 and 2 we present the Feynman graphs representing the contributions up to two-loops and  $\mathcal{O}(\lambda^2)$  to the finite-temperature effective action in the symmetric and broken phases, respectively. In these figures, each external leg means a factor of  $\varphi$ . It is easy to check that the graphs for the broken phase in Fig. 2 are those in Fig. 1 with each external leg shifted by  $\nu$  – of course the  $G^{\alpha\beta}$ 's are different in each set of diagrams, see Eq. (2.25). Notice also that if one were to obtain the graphs in the broken phase from those in the symmetric phase by shifting each external leg by  $\nu$ , terms independent of the field variable  $\varphi$  would appear. These do not appear in the explicit and systematic calculation done above, but can be neglected because they do not contribute to the GLL equations.

### III. STOCHASTIC GLL EQUATIONS

Here we derive an effective GLL equation. It has been shown in several previous works [11, 17, 31, 32, 33] that dissipation is due to non-perturbative effects and cannot be derived from perturbation theory solely due to the appearance of secular terms [34] which lead to the breakdown of perturbation theory well before dissipative effects can be observed. The issues involved in the derivation of the dissipation terms have been extensively discussed and examined, e.g in Refs. [17, 20], to where we refer the interested reader for further details. In particular, in these references it was shown that dissipation naturally emerges when the effects of quasi-particles in a thermal environment are taken into account, for instance, via the self-energy  $\Sigma(q)$ , its real part contributing to the dispersion relation  $E = E(\mathbf{q})$  and its imaginary part to the width  $\Gamma = \Gamma(\mathbf{q})$  of the excitations. In this case, the correlation functions  $G^>$  and  $G^<$  can be written in momentum space as [2]

$$\begin{aligned} G^>(\mathbf{q}, t) &= \frac{1}{E} \left[ (1 + n(E_\Gamma)) e^{-iE_\Gamma t} + n(E_\Gamma^*) e^{iE_\Gamma^* t} \right], \\ G^<(\mathbf{q}, t) &= G^>(\mathbf{q}, -t), \end{aligned} \quad (3.1)$$

where  $E_\Gamma = E - i\Gamma$ , and  $n(E)$  is the Bose-Einstein distribution. In the limit of  $\Gamma = 0$ , one recovers the usual expressions for a noninteracting Bose gas. The explicit expressions for the width  $\Gamma$  and the energy  $E$  can be found

in Refs. [11, 17]. From now on, we shall remove the subindex 0 from  $G^{\alpha\beta}$  to indicate that we are using dressed correlation functions. The fields  $\varphi_+$  and  $\varphi_-$  can be expressed in terms of new variables  $\varphi_c$  and  $\varphi_\Delta$  defined as

$$\varphi_+ = \frac{1}{2} \varphi_\Delta + \varphi_c, \quad \varphi_- = \varphi_c - \frac{1}{2} \varphi_\Delta. \quad (3.2)$$

Using these into the expressions for  $\bar{\Gamma}^{(1)}$  and  $\bar{\Gamma}^{(2)}$ , one can express the result in terms of  $G^{++}$  only, and the effective action can be split into real and imaginary parts,  $\Gamma = \text{Re } \Gamma + i \text{Im } \Gamma$ . The explicit expressions for  $\text{Re } \Gamma$  and  $\text{Im } \Gamma$  for the symmetric phase are given in Ref. [11]. The corresponding expressions for the broken phase can be obtained from those of the symmetric phase by the replacement of  $\varphi_c(x)$  by  $\Phi(x) = \varphi_c(x) + \nu$ , and with the  $G^{++}$  that is appropriate for the broken phase. In view of this, instead of  $\varphi_c$  we will use  $\Phi$  in the following, since when one takes  $\nu = 0$ ,  $\Phi(x) \rightarrow \varphi_c(x)$  and the  $G^{++}$  of the broken phase collapses to the symmetric phase expression when the concomitant change  $m^2 \rightarrow -m^2$  is made.

Given all this, the imaginary part of  $\Gamma[\varphi_\Delta, \Phi]$  can be associated to functional integrations over Gaussian fluctuation fields  $\xi_1$  and  $\xi_2$  by making use of a Hubbard-Stratonovich transformation [11, 30], leading to

$$\Gamma[\varphi_\Delta, \Phi] = -i \ln \int \mathcal{D}\xi_1 P[\xi_1] \int \mathcal{D}\xi_2 P[\xi_2] \exp\{i S_{\text{eff}}[\varphi_\Delta, \Phi, \xi_1, \xi_2]\}, \quad (3.3)$$

with  $S_{\text{eff}}[\varphi_\Delta, \Phi, \xi_1, \xi_2]$  given by

$$S_{\text{eff}}[\varphi_\Delta, \Phi, \xi_1, \xi_2] = \text{Re } \Gamma[\varphi_\Delta, \Phi] + \int d^4x \varphi_\Delta(x) \Phi(x) \xi_1(x) + \int d^4x \varphi_\Delta(x) \xi_2(x), \quad (3.4)$$

and  $P[\xi_1]$  and  $P[\xi_2]$  are Gaussian distribution functions given by

$$P[\xi_1] = N_1^{-1} \exp\left\{-\frac{1}{2} \int d^4x d^4x' \xi_1(x) \left(\frac{\lambda^2}{2} \text{Re}[G^{++}]_{x,x'}^2\right)^{-1} \xi_1(x')\right\}, \quad (3.5)$$

$$P[\xi_2] = N_2^{-1} \exp\left\{-\frac{1}{2} \int d^4x d^4x' \xi_2(x) \left(\frac{\lambda^2}{6} \text{Re}[G^{++}]_{x,x'}^3\right)^{-1} \xi_2(x')\right\}, \quad (3.6)$$

where  $N_1^{-1}$  and  $N_2^{-1}$  are normalization factors, and

$$[G^{++}]_{x,x'}^2 = \int \frac{d^3k}{(2\pi)^3} e^{i\mathbf{k}\cdot(\mathbf{x}-\mathbf{x}')} \int \frac{d^3q}{(2\pi)^3} G^{++}(\mathbf{q}, t-t') G^{++}(\mathbf{q}-\mathbf{k}, t-t'), \quad (3.7)$$

$$[G^{++}]_{x,x'}^3 = \int d^3k e^{i\mathbf{k}\cdot(\mathbf{x}-\mathbf{x}')} \left[ \prod_{j=1}^3 \int \frac{d^3q_j}{(2\pi)^3} G^{++}(\mathbf{q}_j, t-t') \right] \delta(\mathbf{k}-\mathbf{q}_1-\mathbf{q}_2-\mathbf{q}_3). \quad (3.8)$$

Given the distribution functions  $P[\xi_1]$  and  $P[\xi_2]$ , one has that  $\xi_1$  and  $\xi_2$  have zero average and are correlated as

$$\langle \xi_1(x) \xi_1(x') \rangle = \frac{\lambda^2}{2} \text{Re}[G^{++}]_{x,x'}^2, \quad (3.9)$$

$$\langle \xi_2(x) \xi_2(x') \rangle = \frac{\lambda^2}{6} \text{Re}[G^{++}]_{x,x'}^3. \quad (3.10)$$

The fields  $\xi_1$  and  $\xi_2$  in (3.4) act as fluctuation sources for the scalar field configuration  $\varphi$ . While the field  $\xi_1$  couples with both the response field  $\varphi_\Delta$  and with the physical field  $\Phi$ , leading to a multiplicative noise term in the equation of motion for  $\Phi$ , the field  $\xi_2$  gives origin to an additive noise term. As shown recently [21, 35], both two-point correlation functions for  $\xi_1$  and  $\xi_2$  can be related to corresponding dissipation kernels appearing in the effective equation of motion for the scalar background field that can be derived from the effective action (3.4) via (see e.g. [11, 30])

$$\left. \frac{\delta S_{\text{eff}}[\varphi_\Delta, \Phi, \xi_1, \xi_2]}{\delta \varphi_\Delta} \right|_{\varphi_\Delta=0} = 0. \quad (3.11)$$

This leads to a stochastic integro-differential equation given by

$$[\square + m_0^2] \Phi(x) + \frac{\lambda}{3!} \Phi^3(x) + \Phi(x) \mathcal{K}_0[\Phi] + \mathcal{K}_1[\Phi] + \Phi(x) \mathcal{K}_2[\Phi] = \Phi(x) \xi_1(x) + \xi_2(x), \quad (3.12)$$

where  $\mathcal{K}_0[\Phi]$ ,  $\mathcal{K}_1[\Phi]$ , and  $\mathcal{K}_2[\Phi]$  are nonlocal memory kernels given by

$$\mathcal{K}_0[\Phi] = \frac{\lambda}{2} \int \frac{d^3 k}{(2\pi)^3} \frac{1 + 2n(\omega)}{2\omega(\mathbf{k})} \left( 1 + \lambda \int_{-\infty}^t dt' \int \frac{d^3 q}{(2\pi)^3} \text{Im} [G^{++}(\mathbf{q}, t - t')]^2 \right), \quad (3.13)$$

$$\mathcal{K}_1[\Phi] = \frac{\lambda^2}{3} \int d^3 x' \int_{-\infty}^t dt' \Phi(\mathbf{x}', t') \text{Im} [G^{++}]_{x, x'}^3, \quad (3.14)$$

$$\mathcal{K}_2[\Phi] = \frac{\lambda^2}{2} \int d^3 x' \int_{-\infty}^t dt' \Phi^2(\mathbf{x}', t') \text{Im} [G^{++}]_{x, x'}^2. \quad (3.15)$$

We reiterate that this equation is valid for both symmetric and broken phases of the theory.

One problem one has to face here is the renormalization of ultraviolet divergences. Although the renormalization of  $S_{\text{eff}}$  is defined by the usual introduction of counterterms in the initial Lagrangian, the nonlocal memory kernels involve additional complications. In particular, the numerical simulation of nonlocal equations like Eq. (3.12) is a very difficult problem. However, the situation becomes simpler after a series of physically motivated approximations related to spatial and temporal non-localities of the memory kernels. Considering only contributions which are slowly-varying in space and time (this is a valid assumption for systems near equilibrium, when  $\Phi$  is not expected to change considerably with time - quasi-adiabatic approximation [31, 32]), and keeping contributions up to order  $\lambda^2$ , Eq. (3.12) can be put into a GLL form [11]

$$(\square + m_T^2) \Phi(\mathbf{x}, t) + \frac{\lambda_T}{3!} \Phi^3(\mathbf{x}, t) + \eta_1 \Phi^2(\mathbf{x}, t) \dot{\Phi}(\mathbf{x}, t) = \Phi(\mathbf{x}, t) \xi_1(\mathbf{x}, t), \quad (3.16)$$

where  $\eta_1$  is a temperature-dependent dissipation coefficient,  $\lambda_T$  and  $m_T$  (see below) are the renormalized finite-temperature coupling constant and mass, respectively. As explained in [11], the additive noise term,  $\xi_2$ , appearing in Eq. (3.12) drops out at  $\mathcal{O}(\lambda^2)$ , as well as the corresponding dissipation term,  $\sim \eta_2$ . Despite the approximations leading to Eq. (3.16) may imply in a number of issues that need to be accessed for the validity of these approximations (see e.g. [17]), in our numerical simulations we adopted Eq. (3.16) so to make the analysis simpler and so assume the dissipation coefficient  $\eta_1$  as giving an order of estimate for the magnitude of dissipation in the system. An analysis of the validity of Eq. (3.16) based on the basic assumptions leading to it will be checked in Sec. V.B.

The parameters in Eq. (3.16) are given as follows. For the symmetric phase ( $m_0^2 = m^2 > 0$ ) one has in the high-temperature limit  $T/m \gg 1$  and within the validity of perturbation theory in the thermal theory,  $\lambda T/m \ll 1$ , that  $m_T$  and  $\lambda_T$  are given by

$$m_T^2 \stackrel{T \gg m_T}{\simeq} m^2 + \lambda \frac{T^2}{24}, \quad (3.17)$$

$$\lambda_T \simeq \lambda - \frac{3\lambda^2}{16\pi^2} \ln\left(\frac{m}{4\pi T}\right) + \mathcal{O}\left(\lambda^2 \frac{m}{T}\right), \quad (3.18)$$

and the dissipation coefficient  $\eta_1$ , also in the high-temperature limit, given by [11, 17, 31]

$$\eta_1 \stackrel{T \gg m_T}{\simeq} \frac{96}{\pi T} \ln\left(2 \frac{T}{m_T}\right). \quad (3.19)$$

For the broken phase,  $m_0^2 = -m^2 < 0$  and the expression for  $m_T^2$  changes in view of the possibility of symmetry restoration at sufficiently high temperatures. Specifically, the dominant terms are now given by

$$m_T^2 \stackrel{T \gg m_T}{\simeq} -m^2 + \frac{\lambda T^2}{24} + \dots \quad (3.20)$$

From this, one has a critical temperature given by  $T_c^2 = 24m^2/\lambda$ .

#### IV. LATTICE RENORMALIZATION

In our following numerical study, we consider an extended GLL equation, incorporating additive *and* multiplicative noise terms. The time evolution of the field  $\varphi(\mathbf{x}, t)$  at each point in space, which will determine the approach of the condensate  $\langle \varphi \rangle$  to its equilibrium value will be dictated by the following equation:

$$\square \varphi + (\eta_1 \varphi^2 + \eta_2) \dot{\varphi} + \mathcal{V}'_{eff}(\varphi) = \xi_1(\mathbf{x}, t) \varphi + \xi_2(\mathbf{x}, t), \quad (4.1)$$

where  $\eta_1$  and  $\eta_2$ , which can be seen as response coefficients that define time scales for the system and encode the intensity of dissipation, will be taken to be functions of temperature only,  $\eta_a = \eta_a(T)$  ( $a = 1, 2$ ). The functions  $\xi_1(\mathbf{x}, t)$  and  $\xi_2(\mathbf{x}, t)$  represent stochastic (noise) forces, assumed Gaussian and white.

##### A. The need for lattice counterterms

Analytic solutions of Eq. (4.1) are achievable only in very special situations, like in a linear approximation to  $\mathcal{V}_{eff}(\varphi)$ , usually valid only at short times. Complete solutions describing the evolution of the system to equilibrium can be obtained only through extensive numerical simulations. In general, numerical simulations are performed on a discrete spatial lattice of finite length under periodic boundary conditions. However, in performing lattice simulations of Eq. (4.1), one should be careful in preserving the lattice-spacing independence of the results, especially when one is concerned with the behavior of the system in the continuum limit. The equilibrium probability distribution for the field configurations  $\varphi$  that are solutions of Eq. (4.1) is  $P_{eq}[\varphi] = e^{-S[\varphi]}$ , where  $S[\varphi]$  is the Euclidean action. The corresponding partition function is given by the path integral

$$Z[\varphi] = \int \mathcal{D}\varphi e^{-S[\varphi]}. \quad (4.2)$$

The calculation of expectation values and correlation functions of  $\varphi$  with this partition function leads to ultraviolet divergences. In the presence of thermal noise, short and long wavelength modes are mixed during the dynamics, yielding an unphysical lattice spacing sensitivity. The issue of obtaining robust results, as well as the correct ultraviolet behavior, in performing Langevin dynamics was discussed by several authors [36, 37, 38]. The problem, which is not *a priori* evident in the Langevin formulation, is related to the well-known Rayleigh-Jeans ultraviolet catastrophe in classical field theory [39]. The dynamics dictated by Eq. (4.1) is classical, and is ill-defined for large momenta. These *a priori* lattice divergences can be eliminated by renormalizing the potential  $\mathcal{V}_{eff}$  through the addition of appropriate counterterms (notice that these divergences are completely unrelated to the usual ones of the quantum theory). Since the divergent terms are all perturbative, one can identify the appropriate diagrams, subtract their result computed within the *classical theory*, then add the equivalent terms computed within the quantum theory. In our case, this corresponds to substituting the Maxwell-Boltzmann weight by the Bose-Einstein distribution in the momentum integrals for the appropriate divergent terms. Since the theory in three-dimensions is super-renormalizable, only a mass renormalization is required – only the one-loop tadpole and two-loop setting-sun diagrams are divergent. We only require, then, a renormalization of the mass parameter  $m_0^2$  in  $\mathcal{V}_{eff}(\varphi)$ . Using such a renormalized potential in Eq. (4.1) leads to equilibrium solutions  $\varphi$  that are independent of the lattice spacing as we are going to explicitly show below. In practice, this lattice renormalization procedure corresponds to adding finite-temperature counterterms to the original potential  $\mathcal{V}_{eff}(\varphi)$ , which guarantees the correct short-wavelength behavior of the discrete theory as was originally shown by the authors of Ref. [36] within the framework of dimensional reduction in a different context. Furthermore, it assures that the system will evolve to the correct quantum state at large times.

In order to define the notation and the procedure to calculate the loop expansion of the effective potential [40], we first consider the theory in the continuum and switch to the lattice when calculating the loop integrals.

##### B. The classical field effective potential in the continuum: loop corrections

The calculation of the classical three-dimensional loop corrections to the potential starts as usual by introducing a constant field  $\varphi$  through the transformation

$$\phi \rightarrow \phi + \varphi, \quad (4.3)$$

and considering the action

$$\hat{S}[\varphi; \phi] \equiv S[\varphi + \phi] - S[\varphi] - \int d^3x \phi \left. \frac{\partial S[\phi]}{\partial \phi} \right|_{\phi=\varphi}. \quad (4.4)$$

Next, the quadratic terms in  $\hat{S}$  are collected in a “free” action  $\hat{S}_2$ , and the remaining terms in an interacting action,  $\hat{S}_I$ . Then, the effective classical field potential is defined by the expression

$$e^{-\beta V \mathcal{V}_{\text{eff}}[\varphi]} = e^{-\beta V \mathcal{V}[\varphi]} \int \mathcal{D}\phi e^{-\hat{S}[\varphi; \phi]}, \quad (4.5)$$

where  $V$  is the three-dimensional volume. From this expression, one obtains for  $\mathcal{V}_{\text{eff}}[\varphi]$

$$\begin{aligned} \mathcal{V}_{\text{eff}}[\varphi] &= \mathcal{V}[\varphi] - \frac{1}{\beta V} \ln \int \mathcal{D}\phi e^{-\hat{S}_2[\varphi; \phi]} \\ &\quad - \frac{1}{\beta V} \ln \langle e^{-\hat{S}_I[\varphi; \phi]} \rangle, \end{aligned} \quad (4.6)$$

where

$$\langle e^{-\hat{S}_I[\varphi; \phi]} \rangle = \frac{\int \mathcal{D}\phi e^{-\hat{S}_2[\varphi; \phi]} e^{-\hat{S}_I[\varphi; \phi]}}{\int \mathcal{D}\phi e^{-\hat{S}_2[\varphi; \phi]}}. \quad (4.7)$$

The final step is the determination of  $\varphi$  through

$$\frac{d\mathcal{V}_{\text{eff}}[\varphi]}{d\varphi} = 0. \quad (4.8)$$

The action  $\hat{S}_2[\varphi; \phi]$  for bare potential under consideration is given by

$$\hat{S}_2[\varphi; \phi] = \beta \int d^3x \left[ -\frac{1}{2} \phi \nabla^2 \phi + \frac{1}{2} m^2 \phi^2 \right], \quad (4.9)$$

where

$$m^2 = -m_0^2 + \frac{1}{2} \lambda \varphi^2. \quad (4.10)$$

Since  $\varphi$  is constant, the first functional integral in Eq. (4.6) can be easily performed in momentum space, with the result

$$\frac{1}{\beta V} \ln \int \mathcal{D}\phi e^{-\hat{S}_2[\varphi; \phi]} = -\frac{T}{2} \int_k \ln \tilde{G}^{-1}[\varphi; k^2], \quad (4.11)$$

where  $\tilde{G}^{-1}[\varphi; k^2]$  is the inverse of the three-dimensional (classical field) propagator

$$\tilde{G}[\varphi; k^2] = \frac{1}{k^2 + m^2}, \quad (4.12)$$

and  $\int_k \equiv \int \frac{d^3k}{(2\pi)^3}$ . The calculation of the setting-sun diagram requires  $\hat{S}_I$ ,

$$\hat{S}_I[\varphi; \phi] = \beta \int d^3x \left( -\frac{1}{3} \kappa \phi^3 + \frac{1}{4!} \lambda \phi^4 \right), \quad (4.13)$$

with  $\kappa = -\frac{1}{2}\lambda\varphi$ . Expansion of  $e^{-\hat{S}_I}$  in Eq. (4.6) gives

$$\frac{1}{\beta V} \ln \langle e^{-\hat{S}_I[\varphi, \phi]} \rangle_{\text{setting-sun}} = \frac{T^2}{2} \left( \frac{1}{3}\kappa \right)^2 6 H[\varphi], \quad (4.14)$$

where

$$\begin{aligned} H[\varphi] &= \frac{1}{6V} \int d^3x d^3y \langle \phi^3(x) \phi^3(y) \rangle \\ &= \int_k \int_q \tilde{G}[\varphi; k^2] \tilde{G}[\varphi; q^2] \tilde{G}[\varphi; (k+q)^2]. \end{aligned} \quad (4.15)$$

Now, the divergent part of  $\mathcal{V}_{eff}[\varphi]$  is obtained from

$$\left. \frac{d^2 \mathcal{V}_{eff}[\varphi]}{d\varphi^2} \right|_{\text{tadpole+setting-sun}} = \frac{\lambda T}{2} I_{div}[\varphi] - \frac{\lambda^2 T^2}{6} H_{div}[\varphi], \quad (4.16)$$

with

$$I[\varphi] = \int_k \tilde{G}[\varphi; k^2], \quad (4.17)$$

where  $I_{div}[\varphi]$  and  $H_{div}[\varphi]$  represent the divergent parts of  $I[\varphi]$  and  $H[\varphi]$ . Notice that the derivatives of  $H[\varphi]$  with respect to  $\varphi$  lead to finite integrals and hence are irrelevant here. The evaluation of the divergent parts of  $I$  and  $H$  requires a regularization scheme. Since we simulate our GLL equations on a cubic lattice, we shall evaluate these divergent parts by calculating the effective potential on the lattice.

### C. The counterterms for the classical field potential on the lattice

Here we consider the theory on a cubic lattice of volume  $V = L^3$ , with  $L = Na$ , where  $a$  is the lattice spacing and  $N$  is the number of lattice spacings. The coordinates  $x_i$  of the lattice sites are such that  $0 \leq x_i \leq a(N-1)$ . The Laplacian on the lattice,  $\nabla_{latt}^2 \equiv \Delta$ , is defined as

$$\Delta\phi(x) = \frac{1}{a^2} \sum_{i=1}^3 \left[ \phi(x + a\hat{i}) - 2\phi(x) + \phi(x - a\hat{i}) \right], \quad (4.18)$$

where  $\hat{i}$  is the unit cartesian vector indicating the three orthogonal directions of the square lattice. We also impose periodic boundary conditions (PBC) on the fields,

$$\phi(x + aN\hat{i}) = \phi(x), \quad (4.19)$$

and define the Fourier transform  $\tilde{f}(k)$  of a function  $f(x)$  on the lattice as

$$\tilde{f}(k) = a^3 \sum_x e^{-ik \cdot x} f(x). \quad (4.20)$$

Because of the PBC, the allowed lattice momenta form the Brillouin zone  $\mathcal{B}$

$$k_i = \frac{2\pi}{aN} n_i, \quad n_i = 0, 1, 2, \dots, N-1. \quad (4.21)$$

The inverse transform is given by

$$f(x) = \frac{1}{V} \sum_{k \in \mathcal{B}} e^{ik \cdot x} \tilde{f}(k), \quad (4.22)$$

and the momentum summations over the Brillouin zone will be denoted by

$$\frac{1}{V} \sum_{k \in \mathcal{B}} \equiv \int_k. \quad (4.23)$$

Let us now consider the derivation of the effective potential on the lattice. The lattice action is given by

$$S_{latt}[\phi] = a^3 \sum_x \left( -\frac{1}{2} \phi \Delta \phi + \mathcal{V}[\phi] \right), \quad (4.24)$$

where  $\mathcal{V}[\phi]$  is the same as before. The derivation of the effective potential follows the same procedure as in the continuum, leading to expressions for the setting-sun and tadpole graphs as in Eqs. (4.15) and (4.17), but with  $\int_k$  given by the sum over lattice momenta as indicated in Eq. (4.23). What remains to be determined is the lattice propagator corresponding to  $\tilde{G}$ . The lattice propagator  $\tilde{G}_{latt}$  can be obtained from the quadratic action  $\hat{S}_2[\varphi; \phi]$  on the lattice

$$\hat{S}_{2latt}[\varphi; \phi] = a^3 \sum_x \left( -\frac{1}{2} \phi \Delta \phi + \frac{1}{2} m^2 \phi^2 \right), \quad (4.25)$$

with  $m^2$  given by Eq. (4.10). The lattice propagator  $G_{latt}[\varphi; x, y]$  is the inverse of  $(-\Delta + m^2)$ , i.e.

$$a^3 \sum_y (-\Delta + m^2)_{x,y} G_{latt}[\varphi; x, y] = \frac{1}{a^3} \delta_{x,y}, \quad (4.26)$$

where  $\delta_{x,y}$  is the Kronecker delta. Since  $\varphi$  is a constant field, the solution of this equation can be obtained using the Fourier transform of  $G_{latt}[\varphi; x, y]$ , defined as

$$G_{latt}[\varphi; x, y] = \int_k e^{ik \cdot x} \tilde{G}_{latt}[\varphi; k^2]. \quad (4.27)$$

Substituting this into Eq. (4.26), one obtains

$$\tilde{G}_{latt}[\varphi, k^2] = \frac{a^2}{4} \frac{1}{d(\varphi; n_1, n_2, n_3)}, \quad (4.28)$$

where

$$\begin{aligned} d(\varphi; n_1, n_2, n_3) &= \frac{a^2}{4} \left[ 2a^{-2} \sum_{i=1}^3 (1 - \cos ak_i) + m^2 \right] \\ &= \sum_{i=1}^3 \sin^2(\pi n_i / N) + (am/2)^2. \end{aligned} \quad (4.29)$$

One can then write  $I[\varphi]$  for the tadpole diagram as

$$I[\varphi] = \frac{1}{4aN^3} \sum_{n_i=0}^N \frac{1}{d(\varphi; n_1, n_2, n_3)}, \quad (4.30)$$

and the double sum in  $H[\varphi]$  for the setting-sun diagram as

$$H[\varphi] = \frac{1}{64N^6} \sum_{n_i, m_i=0}^{N-1} \frac{1}{d(\varphi; n_1, n_2, n_3) d(\varphi; m_1, m_2, m_3)} \times \frac{1}{d(\varphi; n_1 + m_1, n_2 + m_2, n_3 + m_3)}. \quad (4.31)$$

The divergent parts of the sums above can be isolated in the limits of  $N \rightarrow \infty$  and  $a \rightarrow 0$ . For example, the tadpole sum in the limit of  $N \rightarrow \infty$  can be converted into an integral [36],

$$I[\varphi] = \frac{1}{4a\pi^3} \int_0^\pi d^3x \frac{1}{\sum_i \sin^2 x_i + (am/2)^2} = \frac{1}{4a} \int_0^\infty d\alpha e^{-\alpha(am)^2/4} \left[ e^{-\alpha/2} I_0(\alpha/2) \right]^3, \quad (4.32)$$

where  $I_0$  is the modified Bessel function. In the limit of  $a \rightarrow 0$ , the divergent part of  $I[\varphi]$  is given by [36]

$$I_{div}[\varphi] = \frac{\Sigma}{4\pi a}, \quad (4.33)$$

where  $\Sigma$  is a constant defined by

$$\Sigma = \frac{1}{\pi^2} \int_{-\pi/2}^{+\pi/2} d^3x \frac{1}{\sum_i \sin^2 x_i} \simeq 3.1759. \quad (4.34)$$

It is important to remark here that for  $T < T_c$  it is crucial the use of Eq. (4.8) so that  $m^2 < 0$  in the above expressions. In a more demanding numerical computation,  $H_{div}[\varphi]$  can also be isolated, with the result [36]

$$H_{div}[\varphi] = \frac{1}{16\pi^2} \left[ \ln \left( \frac{6}{aM} \right) + \zeta \right], \quad (4.35)$$

where  $M$  is the renormalization scale and  $\zeta \simeq 0.09$  is another constant appearing in the integrals being evaluated numerically [36].

The renormalized mass in the classical field perturbative loop expansion is obtained as in the case of quantum field theory, i.e. by subtracting the divergent parts of these graphs as indicated in Eq. (4.16):

$$-\frac{1}{2} m^2 \phi^2 \rightarrow -\frac{1}{2} (m^2 + \delta m^2) \phi^2 \equiv -\frac{1}{2} m_R^2 \phi^2, \quad (4.36)$$

where the mass counterterm is given by

$$\delta m^2 = \frac{\lambda T}{2} I_{div}[\varphi] - \frac{\lambda^2 T^2}{6} H_{div}[\varphi]. \quad (4.37)$$

Therefore, we add the following finite-temperature counterterms to our original potential:

$$V_{ct} = \left\{ -\frac{\lambda \Sigma}{8\pi} \frac{T}{a} + \frac{\lambda^2}{96\pi^2} T^2 \left[ \ln \left( \frac{6}{aM} \right) + \zeta \right] \right\} \frac{\phi^2}{2}. \quad (4.38)$$

Note from the above equation that the dependence on the mass scale  $M$  of the lattice conterterm is only logarithmic. So it turns out that results are only very weak dependent on changes of the scale  $M$ . Of course, any change in the renormalization scale  $M$  can be compensated by corresponding changes in the renormalized parameters (which here requires only a change in the renormalized mass, as it is clear from Eq. (4.38)), and as also expected from the renormalization group theory.

## V. NUMERICAL RESULTS

In this Section we present results of extensive numerical simulations for the GLL equation obtained in three spatial dimensions. The numerical methods used to do so are described in the Appendix.

Nowadays the understanding of the relaxation of a field to its equilibrium configuration is of great importance, once there are many natural phenomena that occur out of thermodynamic equilibrium. In order to analyze this behavior, we start by studying the dependence of the solutions on the lattice spacing  $a = L/N$  and then, by introducing the lattice counterterms discussed and derived in the previous section, we show how lattice-independent results can be obtained in Langevin simulations using both standard additive noise and dissipation terms and also in its generalized form, which includes field-dependent (multiplicative) noise and density-dependent dissipation. This is particularly important, since as we have shown in Sec. III, the expected effective equations of motion for background scalar fields result to be in general of the generalized Langevin form.

All results that will be presented here refer to the time dependence of the volume average of the order parameter, defined as

$$\langle \phi(x, y, z, t) \rangle = \frac{1}{N^3} \sum_{ijk} \bar{\phi}_{ijk}^n, \quad (5.1)$$

where  $\bar{\phi}_{ijk}^n$  is the average over a large number  $N_r$  of independent noise realizations,

$$\bar{\phi}_{ijk}^n = \frac{1}{N_r} \sum_{r=1}^{N_r} \phi_{ijk}^n. \quad (5.2)$$

In all our numerical Langevin simulations, we consider  $N_r$  between 20 and 100. As usual, lattices with larger values of  $L$  require relatively less realizations over the noise. We have considered and tested different lattice sizes to ensure the robustness of all numerical results.

### A. The problem of lattice dependence in the generalized GLL approach

As discussed in the previous section, the simulation of equations with noise, being classical by nature, leads to the appearance of Rayleigh-Jeans ultraviolet divergences at long times when simulating the equation on a discrete lattice. These divergences manifest themselves in the form of lattice-spacing dependence of the equilibrium solutions. We can show that by just considering the easiest nonequilibrium evolution, which is the one of relaxation to the equilibrium vacuum state with initial conditions away from it. In Figs. 3 and 4 we show the corresponding dynamics for the scalar field expectation value,  $\langle \phi(x, y, z, t) \rangle$  defined in Eqs. (5.1) and (5.2), in the broken symmetry case,  $T < T_c$ , with the critical temperature  $T_c$  extracted from the finite-temperature effective potential.

The initial state for the field in the simulations for the broken phase was taken around the inflexion (or spinodal) point of the finite-temperature (Ginzburg-Landau) potential,  $\phi_{\text{infl}}$ , defined by

$$\left. \frac{d^2 V_{\text{eff}}(\phi, T)}{d\phi^2} \right|_{\phi=\phi_{\text{infl}}} = 0. \quad (5.3)$$

In Fig. 3 we show results for the standard Langevin equation (1.1), while Fig. 4 displays results for the generalized case. The parameter values considered for the temperature and dissipation terms  $\eta_1$  and  $\eta_2$ , in units of the scalar field mass, were  $T/m = m\eta_1 = \eta_2/m = 1$ , while the quartic coupling constant was chosen to be  $\lambda = 0.25$ . The scale  $M$  is taken as  $M/m = 1$ . These values suffice for our purposes of just demonstrating the lattice dependence problem in Langevin simulations. In Figs. 3 and 4 the number of lattice points and the time stepsize were kept constant,  $N = 64$  and  $\delta t = 0.01$  (in units of the scalar field mass), respectively, while the lattice spacing,  $m\delta x \equiv a = L/N$ , was varied.

It is clear that the solutions shown in Figs. 3 and 4 are not stable as the lattice spacing is modified. As discussed previously, this problem can be traced to the fact that the equilibrium value of the quantity  $\bar{\phi}_{ijk}$  gives the classical average

$$\bar{\phi}_{ijk} = \frac{\int D\phi \phi_{ijk} e^{-\beta V(\phi)}}{\int D\phi e^{-\beta V(\phi)}}, \quad (5.4)$$

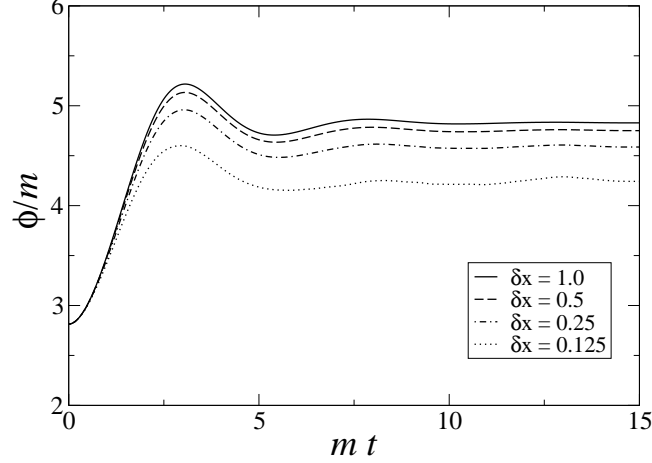


Figure 3: Solution of the standard GLL equation (1.1) using the leap frog algorithm for different lattice spacings.

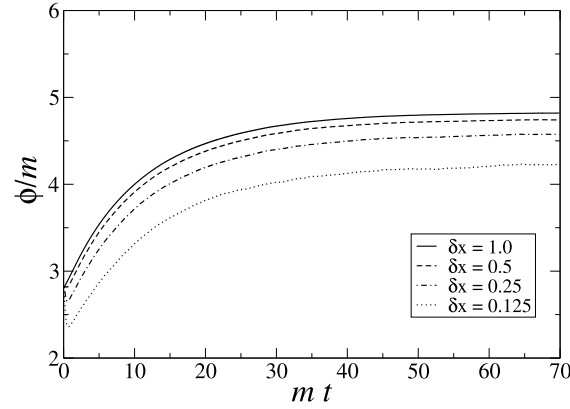


Figure 4: Solution of the GLL equation with both additive and multiplicative noise and dissipation terms using the leap frog algorithm for different lattice spacings. The other parameters are the same as in Fig. 3.

an ultraviolet divergent quantity. Thus, stable equilibrium solutions of the GLL equation, i.e., solutions not sensitive to lattice spacing, can only be obtained by the introduction of the appropriate counterterms in the effective potential in order to eliminate these divergences. These counterterms are the ones derived in the previous section and given by Eq. (4.38).

In Figs. 5 and 6 we present the results of the simulations including the counterterms. As we can see, equilibrium solutions that are independent of lattice spacing are obtained.

For the standard GLL equation this was shown extensively in a series of previous papers [37], but we are not aware of the same demonstration for the case including multiplicative noise terms. From the results shown in Figs. 5 and 6 we can also immediately draw a couple of interesting conclusions. The first is that even though the counterterms used were calculated with an equilibrium partition function, thus ensuring lattice-spacing independence only in equilibrium (long times) situations, the results for short times show only small lattice-spacing dependence. Second, we can notice that the relaxation time scales to the vacuum state is about the same in all cases. Another observation we can make based on the results shown in Figs. 5 and 6 is that the dynamics with multiplicative noise and dissipation terms can be quite different from that driven by additive noise only. In particular, notice from Fig. 6 that the relaxation time to the vacuum state with the generalized GLL equation is much longer than the one with just additive noise, even

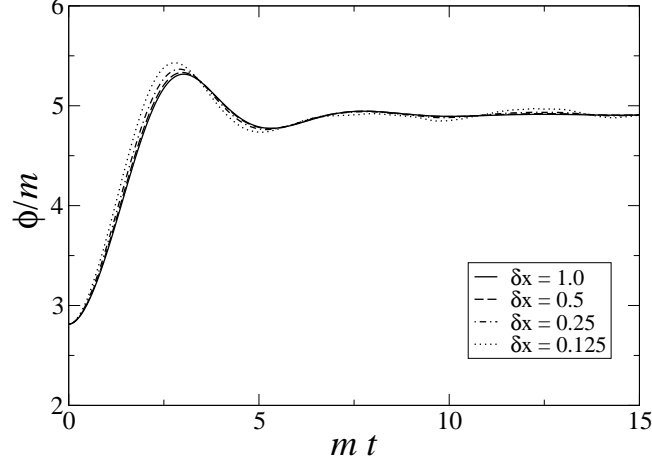


Figure 5: Solution of the standard GLL equation using the leap frog algorithm for different lattice spacings and including the renormalization counterterms.

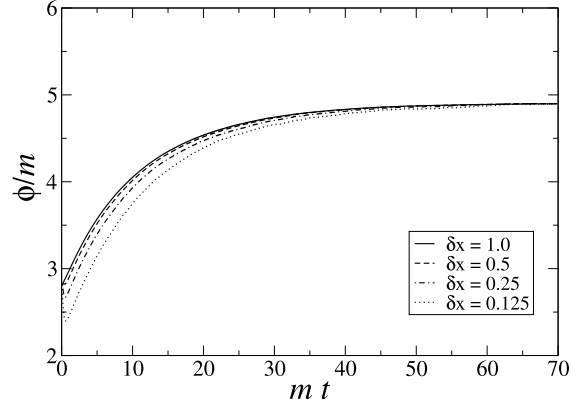


Figure 6: Solution of the GLL equation with both additive and multiplicative noise, and dissipation terms and including the renormalization counterterms.

though the magnitude of the dissipation coefficients (in the dimensionless units in terms of the field mass  $m$ ) are of order one. Also, no oscillation of  $\langle\phi\rangle$  is seen in Fig. 6. When we consider the typical magnitude of the multiplicative dissipation coefficient obtained within the local approximation, Eq. (3.19), which is about two orders of magnitude larger than the one used in the example of Fig. 6, we expect a much longer relaxation time for the scalar condensate. This is typical of a regime of strong overdamping, implicit in the derivation of the local equation (3.16) [17]. As we are going to see next, the study of Eq. (3.16) on the lattice will provide us a unique way of accessing the limit of validity of the approximations used in order to arrive at that equation, thus generalizing to a much more realistic situation the simplified studies performed in Ref. [17].

## B. Simulation results and tests of validity

Finally, we present results of simulations for the GLL in the symmetric and broken cases. Let us first study the broken case to complement the results presented for the phenomenological parameters considered e.g. in Fig. 6.

Considering Eq. (3.16), with dissipation coefficient given by Eq. (3.19), we show in Fig. 7 results obtained for different values of temperature  $T < T_c$  for a cubic lattice with  $N = 64$  and  $L = 32$ . The stepsize in time is  $\delta t = 0.01$  (as before, we normalize all quantities by the scalar field mass  $m$ ) and in all results to be presented henceforth, the proper lattice counterterms to the effective potential, Eq. (4.38), were taken into account. The initial value for the field in all cases was around the inflexion (spinodal) point,  $\phi_{\text{infl}}$ , Eq. (5.3), at each respective temperature.

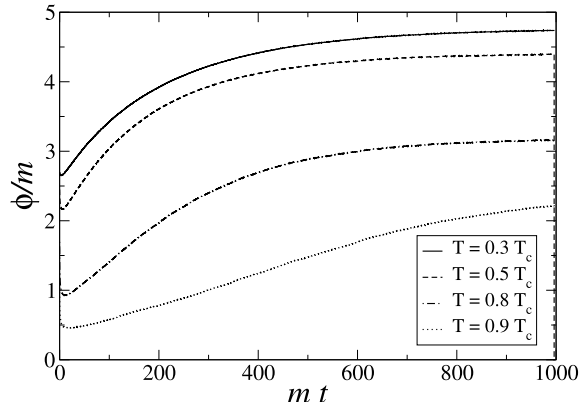


Figure 7: Solutions for different values of temperature of the microscopically derived effective equation of motion in the broken phase.

The curves displayed in Fig. 7 show the large relaxation time to achieve the equilibrium vacuum state due to the large magnitude of the multiplicative dissipation term  $\eta_1$ , as anticipated in the previous subsection. We can also see from the results of Fig. 7 that the dynamics for the scalar field condensate is mostly overdamped all the way to the equilibrium state, except by some very small transient nonequilibrium evolution around the initial time. This seems to support the adiabatic approximation (of slowly varying field) used to derive the local effective equation of motion for the condensate field and used to obtain e.g. Eq. (3.16) from the full nonlocal result, Eq. (3.12). It shows that the lattice evolution of the nonhomogeneous field  $\phi(\mathbf{x}, t)$  can be much less restrictive with respect to the adiabatic approximation than the one for the homogeneous field approximation considered in Ref. [17]. In this reference it was shown that the dynamics for a homogeneous field could only be overdamped in the high-temperature, high-amplitude regime, and when the scalar field is coupled to a large number of other scalar fields. The results shown here seem to indicate that these restrictions are not all necessary for an overdamped dynamical regime. As for the other conditions used to derive Eq. (3.12), and then the local approximation (3.16), are concerned, e.g. the amplitude expansion for the field, and the high-temperature approximation used in the derivation of the dissipation coefficient (3.19), these are clearly valid for the parameters considered in our case to obtain Fig. 7. Other values of coupling constant  $\lambda$  and initial field value can easily be found to satisfy these conditions as well.

As for the basic approximation used in all calculations shown in Sec. II, i.e., the loop expansion, our lattice simulations also offer a simple test to check its validity. Recall that the loop expansion is valid provided that the (vacuum and thermal) fluctuations at some given temperature are sufficiently small, in which case the classical field configuration used to derive the functional partition function is close enough to the solution that extremizes the classical action. This is not so if the fluctuations have large amplitudes. In Ref. [41] it was shown, for the broken potential, that these fluctuations should have an amplitude not larger than the inflexion point of effective potential and in that reference, fluctuations were modeled as subcritical bubbles (see also [42]) in order to compute their amplitude, or actually their root mean square (RMS) amplitude. The equivalent quantity that can be considered here is the RMS variance of the field on the lattice, defined as

$$\phi_{\text{RMS}} = \sqrt{\langle \phi^2 \rangle - \langle \phi \rangle^2}, \quad (5.5)$$

where the averages are on the lattice and taken analogously as in Eqs. (5.1) and (5.2).

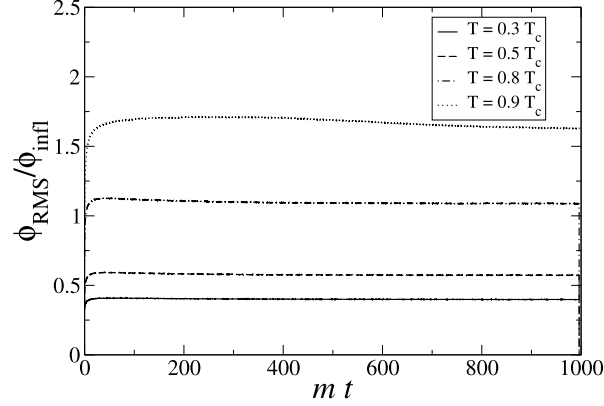


Figure 8: The RMS amplitude of fluctuations (normalized by the equilibrium  $\phi_{\text{infl}}$ ) as a function of time.

In Fig. 8 we shown  $\phi_{\text{RMS}}(t)$  for the four temperatures considered in Fig. 7. We see that  $\phi_{\text{RMS}} > \phi_{\text{infl}}$  already for  $T \gtrsim 0.7T_c$ , beyond which thermal fluctuations become too large and the loop expansion used to derive Eq. (3.12) is no longer valid.

It is important to notice that the thermalization of the field in our simulations is a rather fast process, happening typically in a very short time,  $t_{\text{therm}} \sim 0.5/m$ , which is mostly due to the large dissipation coefficient (3.19) coming from our calculations and subsequent approximations. During the transient initial time given by  $t_{\text{therm}}$ , where it is mostly out of equilibrium, the background field quickly reaches a thermal equilibrium stationary state. Thus, the thermalization time in a Langevin simulation is a rather quick process, even though the system is still evolving in time. The actual equilibration time for the field in its vacuum state happens in a much longer time, as observed in our simulations.

Next, we consider the symmetric phase (with positive mass term in the potential). Results for the symmetric case are presented in Fig. 9. For this case, we considered parameter values satisfying the perturbative expansion ( $m^2 \gg \lambda\phi^2/2$ ,  $\lambda T/m < 1$ ) and high-temperature approximation, given by  $\lambda = 0.01$ ,  $T/m = 5$ , and initial field amplitudes  $\phi_0 = 5m$  and  $\phi_0 = 10m$ , such that we could compare to similar values used in Ref. [17] in order to probe the overdamped dynamical regime for the scalar field. The lattice parameters are the same,  $N = 64$ ,  $L = 32$ , as well as the stepsize in time,  $\delta t = 0.01$ .

Notice from Fig. 9 that the dynamics is again mostly overdamped, with the relaxation time for the field increasing with the initial field amplitude, thus seeming to support the results of Ref. [17] that showed that the overdamped regime is more favorable the larger the field amplitude is. As for the broken case, we can again probe the validity of the loop expansion used to derive the effective evolution equation for the field. Since in this case the potential has always a positive definite curvature, we use the conservative criterion that the perturbative expansion is valid for fluctuations dominated by the quadratic term of the effective potential, i.e.,

$$\phi_{\text{fluct}} \lesssim \phi_{\text{max}} , \quad (5.6)$$

where

$$\phi_{\text{max}} = \sqrt{12 \frac{m_T^2}{\lambda_T}} , \quad (5.7)$$

with  $m_T^2$  and  $\lambda_T$  given by Eqs. (3.17) and (3.18), respectively. In Fig. 10 we show the RMS amplitude of fluctuations of the field on the lattice for the two cases shown in Fig. 9. Since, from Eq. (5.7) and the parameters used,  $\phi_{\text{max}} \sim 34m$ , both cases shown in Fig. 9 comfortably satisfy the criterion (5.6) for the validity of the loop expansion.

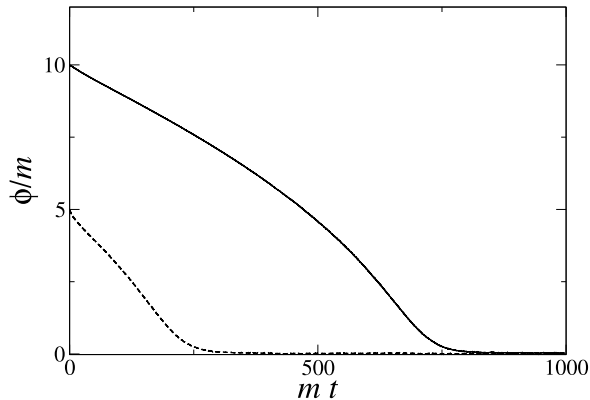


Figure 9: Solutions of the microscopically derived effective equation of motion in the symmetric phase for two different values of initial field amplitude.

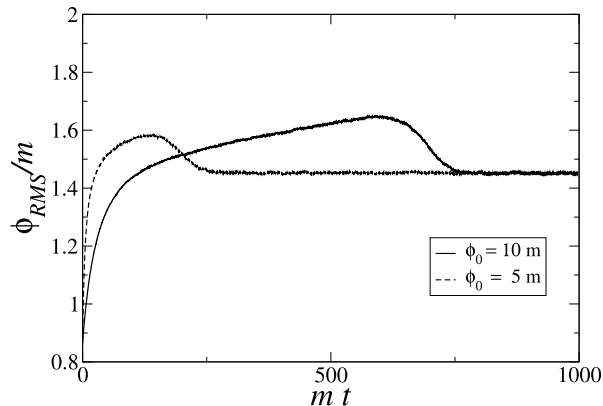


Figure 10: The RMS amplitude of fluctuations of the field on the lattice for the two values of initial field amplitudes shown in Fig. 9 for the symmetric case.

## VI. CONCLUSIONS

In this work we have studied several important aspects regarding the dynamics of a scalar field background configuration in both symmetric and broken symmetry phases. It has been long recognized that the effective evolution equation for the field can be of a complicated form. From the analogy with standard Langevin equations for the study of the approach to equilibrium, the microscopically derived effective evolution equation allows for the presence of similar additive noise and dissipation terms, but also for multiplicative (field-dependent) noise and dissipation terms. Although equations of motion of the standard Langevin form (with only additive noise and dissipation) have been extensively studied in the literature, its generalized form, which includes the multiplicative noise and dissipation terms, still demands extensive studies. Here we have performed a number of numerical simulations with these equations on a cubic lattice. We have also called the attention to another issue frequently overlooked in the literature: the necessity of adding lattice renormalization counterterms to cancel Rayleigh-Jeans divergences of the corresponding

classical theory, in order to produce sensible results from Langevin simulations. We have shown that the same lattice counterterms that are required for the standard Langevin simulations also work for the generalized Langevin equations, producing lattice-independent equilibrium quantities, and also minimizing the dependence of the dynamics on the lattice parameters.

In our studies of the generalized Langevin equation for both the broken and symmetric cases, with a typical value of dissipation coefficient as produced from a local and high-temperature approximation for the effective equation of motion for the background scalar field, we have shown that the dynamics produced is overdamped. Moreover, we were able to test some of the approximations used to derive these equations, such as the validity of the loop expansion. This allowed us to explicitly test some of the hypotheses and results obtained in Ref. [17], studied there only for the homogeneous field approximation.

One interesting and important problem that still remains, though beyond the objectives set for the present work, is the study of the validity of the approximation of transforming the complicated nonlocal (non-markovian) equations of motion obtained through a microscopic derivation (via the Schwinger-Keldysh real-time formalism for the effective action) into the local form used in the simulations performed for this study. This is a notoriously difficult problem due to the oscillatory nature of the nonlocal kernels appearing in the full effective equation of motion, which leads to uncontrollable numerical behavior in simulations. We are currently studying viable numerical strategies to deal with this problem and to fully access the local approximation for the equations, as well as the differences in its dynamics as compared to the nonlocal equations. Results in this direction will be presented in a future publication.

### Acknowledgments

E.S.F. would like to thank T. Kodama, T. Koide, A. J. Mizher and L. F. Palhares for discussions on related matters. This work was partially supported by CAPES, CNPq, FAPERJ, FAPESP and FUJB/UFRJ.

### Appendix A: THE GLL EQUATION ON THE LATTICE

The equation to be solved on the lattice is

$$\frac{\partial^2 \phi}{\partial t^2} - \nabla^2 \phi + \eta_1 \phi^2 \frac{\partial \phi}{\partial t} + \eta_2 \frac{\partial \phi}{\partial t} + \mathcal{V}'_{\text{eff}}(\phi) = \phi \xi_1 + \xi_2. \quad (\text{A1})$$

We solve the GLL equation on the lattice with periodic boundary conditions (PBC). When we insert the system in a box,  $\phi$  acquires a discrete form  $\phi_{ijk}^n$ , where  $t = n\Delta t$  with  $n = 0, 1, 2, \dots$ ,  $x = ia$ ,  $y = ja$  and  $z = ka$ , being  $a$  the lattice spacing  $a = \frac{L}{N}$ . Using PBC we have

$$\begin{aligned} \phi_{N+1jk}^n &= \phi_{1jk}^n; \phi_{iN+1k}^n = \phi_{i1k}^n; \phi_{ijN+1}^n = \phi_{ij1}^n, \\ \phi_{N+1N+1k}^n &= \phi_{11k}^n; \phi_{N+1jN+1}^n = \phi_{1j1}^n; \phi_{iN+1N+1}^n = \phi_{i11}^n, \\ \phi_{N+1N+1N+1}^n &= \phi_{111}^n; \phi_{0jk}^n = \phi_{Njk}^n; \phi_{i0k}^n = \phi_{iNk}^n, \\ \phi_{ij0}^n &= \phi_{ijN}^n; \phi_{i00}^n = \phi_{iNN}^n; \phi_{0j0}^n = \phi_{NjN}^n, \\ \phi_{00k}^n &= \phi_{NNk}^n; \phi_{000}^n = \phi_{NNN}^n. \end{aligned} \quad (\text{A2})$$

Firstly we write the Laplacian

$$\begin{aligned} \nabla^2 \phi_{ijk}^n &= \frac{\partial^2 \phi_{ijk}^n}{\partial^2 x} + \frac{\partial^2 \phi_{ijk}^n}{\partial^2 y} + \frac{\partial^2 \phi_{ijk}^n}{\partial^2 z} \\ &= \frac{1}{a} \left[ \left( \frac{\phi_{i+1jk}^n - \phi_{ijk}^n}{a} \right) - \left( \frac{\phi_{ijk}^n - \phi_{i-1jk}^n}{a} \right) \right. \\ &\quad + \left( \frac{\phi_{ij+1k}^n - \phi_{ijk}^n}{a} \right) - \left( \frac{\phi_{ijk}^n - \phi_{ij-1k}^n}{a} \right) \\ &\quad + \left. \left( \frac{\phi_{ijk+1}^n - \phi_{ijk}^n}{a} \right) - \left( \frac{\phi_{ijk}^n - \phi_{ijk-1}^n}{a} \right) \right] \\ &= \frac{1}{a^2} [\phi_{i+1jk}^n + \phi_{ij+1k}^n + \phi_{ijk+1}^n \\ &\quad - 6\phi_{ijk}^n + \phi_{i-1jk}^n + \phi_{ij-1k}^n + \phi_{ijk-1}^n]. \end{aligned} \quad (\text{A3})$$

For simplicity, we introduce the compact notation

$$\nabla^2 \phi_{ijk}^n = (L\phi)_{ijk}^n . \quad (\text{A4})$$

In addition, we divide the time in  $n$  steps,  $t = n\Delta t$ , with  $n = 0, 1, 2, \dots$ . With respect to the discretization of the time derivatives, we use the leapfrog approximation method, where the algorithm is defined by the following iteration scheme:

$$\begin{aligned} \frac{\partial \phi_n}{\partial t} &= \dot{\phi}_n = \frac{1}{2} \left( \dot{\phi}_{n+1/2} + \dot{\phi}_{n-1/2} \right) , \\ \dot{\phi}_{n+1/2} &= \frac{1}{\Delta t} (\phi_{n+1} - \phi_n) , \\ \frac{\partial^2 \phi_n}{\partial t^2} &= \ddot{\phi}_n = \frac{1}{\Delta t} \left( \dot{\phi}_{n+1/2} - \dot{\phi}_{n-1/2} \right) . \end{aligned} \quad (\text{A5})$$

Now we rewrite (A1) in terms of discrete field  $\phi_{ijk}^n$

$$\frac{\partial^2 \phi_{ijk}^n}{\partial t^2} - \nabla^2 \phi_{ijk}^n + \eta_1 (\phi_{ijk}^n)^2 \frac{\partial \phi_{ijk}^n}{\partial t} + \eta_2 \frac{\partial \phi_{ijk}^n}{\partial t} + \mathcal{V}'_{\text{eff}}(\phi_{ijk}^n) = \phi_{ijk}^n \xi_1 + \xi_2 . \quad (\text{A6})$$

Using the discretized quantities derived above we obtain

$$\begin{aligned} \frac{1}{\Delta t} \left( \dot{\phi}_{ijk}^{n+1/2} - \dot{\phi}_{ijk}^{n-1/2} \right) &= (L\phi)_{ijk}^n - \eta_1 (\phi_{ijk}^n)^2 \frac{1}{2} \left( \dot{\phi}_{ijk}^{n+1/2} + \dot{\phi}_{ijk}^{n-1/2} \right) \\ &\quad - \eta_2 \frac{1}{2} \left( \dot{\phi}_{ijk}^{n+1/2} + \dot{\phi}_{ijk}^{n-1/2} \right) \\ &\quad - \mathcal{V}'_{\text{eff}}(\phi_{ijk}^n) + \phi_{ijk}^n \xi_1 + \xi_2 , \end{aligned} \quad (\text{A7})$$

$$\begin{aligned} \dot{\phi}_{ijk}^{n+1/2} - \dot{\phi}_{ijk}^{n-1/2} &= (L\phi)_{ijk}^n \Delta t - \frac{1}{2} \left[ \eta_1 (\phi_{ijk}^n)^2 + \eta_2 \right] \dot{\phi}_{ijk}^{n+1/2} \Delta t \\ &\quad - \frac{1}{2} \left[ \eta_1 (\phi_{ijk}^n)^2 + \eta_2 \right] \dot{\phi}_{ijk}^{n-1/2} \Delta t \\ &\quad - \mathcal{V}'_{\text{eff}}(\phi_{ijk}^n) \Delta t + \phi_{ijk}^n \xi_1 \Delta t + \xi_2 \Delta t . \end{aligned} \quad (\text{A8})$$

The equation that we solve by iteration is

$$\begin{aligned} \left\{ 1 + \frac{1}{2} \left[ \eta_1 (\phi_{ijk}^n)^2 + \eta_2 \right] \Delta t \right\} \dot{\phi}_{ijk}^{n+1/2} &= \left\{ 1 - \frac{1}{2} \left[ \eta_1 (\phi_{ijk}^n)^2 + \eta_2 \right] \Delta t \right\} \dot{\phi}_{ijk}^{n-1/2} + (L\phi)_{ijk}^n \Delta t \\ &\quad - \mathcal{V}'_{\text{eff}}(\phi_{ijk}^n) \Delta t + \phi_{ijk}^n \xi_1 \Delta t + \xi_2 \Delta t . \end{aligned} \quad (\text{A9})$$

In a compact notation we have

$$\begin{aligned} \dot{\phi}_{ijk}^{n+1/2} &= \frac{1}{\Xi} \left[ \dot{\phi}_{ijk}^{n-1/2} \Theta + (L\phi)_{ijk}^n \Delta t - \mathcal{V}'_{\text{eff}}(\phi_{ijk}^n) \Delta t \right. \\ &\quad \left. + \phi_{ijk}^n \xi_1 \Delta t + \xi_2 \Delta t \right] , \end{aligned} \quad (\text{A10})$$

where

$$\begin{aligned} \Xi &= 1 + \frac{1}{2} \left[ \eta_1 (\phi_{ijk}^n)^2 + \eta_2 \right] \Delta t , \\ \Theta &= 1 - \frac{1}{2} \left[ \eta_1 (\phi_{ijk}^n)^2 + \eta_2 \right] \Delta t . \end{aligned} \quad (\text{A11})$$

To update the field we make

$$\phi_{ijk}^{n+1} = \phi_{ijk}^n + \Delta t \dot{\phi}_{ijk}^{n+1/2} . \quad (\text{A12})$$

Finally, on the lattice the noise terms are modelled to satisfy the discretized fluctuation-dissipation relation ( $i = 1, 2$  denote one of the two noise and respective dissipation terms appearing in the generalized GLL equation (4.1))

$$\langle \xi_{i,n} \xi_{j,n'} \rangle = 2\eta_i T \delta_{i,j} \delta_{n,n'} / (a^3 \Delta t) , \quad (\text{A13})$$

so that its amplitude that can be written as

$$\xi_{i,n} = \sqrt{\frac{2\eta_i T}{a^3 \Delta t}} G_{i,n} , \quad (\text{A14})$$

where  $G_{i,n}$  is obtained from a zero-mean unit-variance Gaussian.

Finally, since we are dealing with multiplicative noise in a Langevin equation, there is a well-known ambiguity in the discretization of time [43]. This ambiguity is manifest whenever there are multiplicative noises and they are delta-correlated in time (i.e., they are Markovian, like in the approximation we have adopted in our simulations), and leads to the two most common types of discretization procedures, the one by Ito and the one by Stratonovich [44]. The leapfrog scheme shown in Eq. (A10) corresponds to Ito's prescription. The ambiguity can be seen when one discretizes the (Markovian) multiplicative noise term. Notice from Eq. (A14) that the noise terms in Eq. (A10) are actually of order  $(\Delta t)^{1/2}$ , instead of order  $\Delta t$  as the remaining terms. So, the multiplicative noise term needs to be re-expanded up to the next order in  $\Delta t$ . This can be performed when one writes the discretized form for the multiplicative noise term using the Riemann formula

$$\int_t^{t+\Delta t} \phi(\mathbf{x}, t') \xi_1(\mathbf{x}, t') dt' = [(1 - \alpha)\phi(\mathbf{x}, t) + \alpha\phi(\mathbf{x}, t + \Delta t)] \chi_1(\mathbf{x}, t) , \quad (\text{A15})$$

where  $0 \leq \alpha \leq 1$ , with the Stratonovich prescription corresponding to  $\alpha = 1/2$ , while Ito's corresponds to for  $\alpha = 0$  [44]. In (A15)  $\chi_1(\mathbf{x}, t)$  is a new Gaussian stochastic process described by (in discretized form)

$$\langle \chi_{1,n} \chi_{1,n'} \rangle = 2\eta_1 T \delta_{n,n'} \Delta t / a^3 . \quad (\text{A16})$$

Using Eq. (A15) back in the leapfrog equation (A10) and re-expanding it to the next order in the multiplicative noise term one finds that in the Stratonovich interpretation there is an additional correction term to the leapfrog equation (A10) of order  $\alpha \dot{\phi}_{ijk}^{n-1/2} \chi_1 \Delta t \Theta / \Xi^2$ , which is already an order  $(\Delta t)^{1/2}$  higher than the remaining terms in that equation. We have explicitly checked in all our simulations that this is a negligible correction for our results, and so we have adopted the Ito's prescription, i.e. Eq. (A10). Notice that this might not be the case would we be working with first order in time derivative equations, in which case large corrections due to the difference between Ito's and Stratonovich's interpretations can arise [45]). For a recent discussion on different prescriptions in the context of the relativistic Brownian motion, see e.g. Ref. [46].

- 
- [1] L. Dolan and R. Jackiw, Phys. Rev. D **9**, 3320 (1974).
  - [2] M. Le Bellac, *Thermal Field Theory* (Cambridge University Press, 2000).
  - [3] U. Kraemmer and A. Rebhan, Rept. Prog. Phys. **67**, 351 (2004).
  - [4] J. O. Andersen and M. Strickland, Annals Phys. **317**, 281 (2005).
  - [5] Proceedings of Quark Matter 2005, Nucl. Phys. A **774**, 1-968 (2006).
  - [6] J. Rafelski and J. Letessier, Phys. Rev. Lett. **85**, 4695 (2000).
  - [7] A. Dumitru and R. D. Pisarski, Nucl. Phys. A **698**, 444 (2002). O. Scavenius, A. Dumitru and A. D. Jackson, Phys. Rev. Lett. **87**, 182302 (2001).
  - [8] R. D. Pisarski, Phys. Rev. D **62**, 111501 (2000); A. Dumitru and R. D. Pisarski, Phys. Lett. B **504**, 282 (2001).
  - [9] J. Randrup, Phys. Rev. Lett. **92**, 122301 (2004); nucl-th/0406031; V. Koch, A. Majumder and J. Randrup, Phys. Rev. C **72**, 064903 (2005).
  - [10] E. S. Fraga and G. Krein, Phys. Lett. B **614**, 181 (2005).

- [11] M. Gleiser and R. O. Ramos, Phys. Rev. D **50**, 2441 (1994).
- [12] C. Greiner and B. Muller, Phys. Rev. D **55**, 1026 (1997).
- [13] D. H. Rischke, Phys. Rev. C **58**, 2331 (1998).
- [14] O. Scavenius, A. Dumitru, E. S. Fraga, J. T. Lenaghan and A. D. Jackson, Phys. Rev. D **63**, 116003 (2001).
- [15] E. S. Fraga, T. Kodama, G. Krein, A. J. Mizher and L. F. Palhares, Nucl. Phys. A **785**, 138 (2007).
- [16] E. S. Fraga, G. Krein and A. J. Mizher, Phys. Rev. D **76**, 034501 (2007).
- [17] A. Berera, M. Gleiser and R. O. Ramos, Phys. Rev. D **58**, 123508 (1998).
- [18] R. O. Ramos and F. A. R. Navarro, Phys. Rev. D **62**, 085016 (2000).
- [19] A. Berera and R. O. Ramos, Phys. Rev. D **63**, 103509 (2001).
- [20] A. Berera and R. O. Ramos, Phys. Rev. D **71**, 023513 (2005).
- [21] A. Berera, I. G. Moss and R. O. Ramos, Phys. Rev. D **76**, 083520 (2007).
- [22] N. D. Antunes, P. Gandra and R. J. Rivers, Phys. Rev. D **71**, 105006 (2005).
- [23] R. L. S. Farias, PhD Thesis, Instituto de Física Teórica, Universidade Estadual Paulista, Brazil (in portuguese).
- [24] R.L.S. Farias, N.C. Cassol-Seewald, G. Krein, R. O. Ramos, Nucl. Phys. A **782**, 33 (2007).
- [25] S. Coleman, *Aspects of Symmetry* (Cambridge University Press, 1985).
- [26] J. Schwinger, Math. Phys. **2**, 407 (1961); L.V. Keldysh, Zh. Eksp. Teor. Fiz. **47**, 1515 (1964); A. Niemi and G. Semenoff, Ann. Phys. (N.Y.) **152**, (1984); Nucl. Phys. **B230**, 181 (1984).
- [27] K. Chou, Z. Su, B. Hao and L. Yu, Phys. Rep. **118**, 1 (1985).
- [28] I. L. Buchbinder, S. D. Odintsov and I. L. Shapiro, *Effective Action in Quantum Gravity* (Institute of Physics Publishing, Bristol, 1992).
- [29] N.P. Landsman and Ch.G. van Weert, Phys. Rep. **145**, 141 (1987).
- [30] M. Morikawa, Phys. Rev. D **33**, 3607 (1986).
- [31] A. Hosoya and M. Sakagami, Phys. Rev. **D29**, 2228 (1984).
- [32] M. Morikawa and M. Sasaki, Phys. Lett. **165B**, 59 (1985).
- [33] A. Ringwald, Ann. Phys. (NY) **177**, 129 (1987); Phys. Rev. **D36**, 2598 (1987).
- [34] D. Boyanovsky, H. J. de Vega, R. Holman, D.-S. Lee and A. Singh, Phys. Rev. **D51**, 4419 (1995).
- [35] J. Yokoyama, Phys. Rev. **D70**, 103511 (2004).
- [36] K. Farakos, K. Kajantie, K. Rummukainen and M. E. Shaposhnikov, Nucl. Phys. B **425**, 67 (1994); *ibid.* B **442**, 317 (1995).
- [37] J. Borrill and M. Gleiser, Nucl. Phys. B **483**, 416 (1997); L. M. A. Bettencourt, S. Habib and G. Lythe, Phys. Rev. D **60**, 105039 (1999); C. J. Gagne and M. Gleiser, Phys. Rev. E **61**, 3483 (2000); L. M. A. Bettencourt, K. Rajagopal, and J. V. Steele, Nucl. Phys. A **693**, 825 (2001).
- [38] E. S. Fraga, G. Krein and R. O. Ramos, AIP Conf. Proc. **814**, 621 (2006); E. S. Fraga, Eur. Phys. J. A **29**, 123 (2006).
- [39] G. Parisi, Statistical Field Theory (Addison-Wesley, New York, 1988).
- [40] R. Jackiw, Phys. Rev. D **9**, 1686 (1974).
- [41] M. Gleiser and R. O. Ramos, Phys. Lett. **B300**, 271 (1993).
- [42] M. Gleiser, R. C. Howell and R. O. Ramos, Phys. Rev. **E65**, 036113 (2002).
- [43] P. Arnold, Phys. Rev. E **61**, 6091 (2000).
- [44] C. W. Gardiner, *Handbook of Stochastic Methods for Physics, Chemistry and the Natural Sciences* (Springer, 2004).
- [45] F. Sagués, J. M. Sancho and J. Garcia-Ojalvo, Rev. Mod. Phys. **79**, 829 (2007).
- [46] T. Koide and T. Kodama, arXiv:0710.1904 [hep-th].